Yu Wenxi (Orcid ID: 0000-0003-0911-2706)

1st Revision – June 18th

Allele-Specific Editing of a Dominant *SCN8A* Epilepsy Variant Protects against Seizures and Lethality in a Murine Model

Wenxi Yu, PhD[1], Sophie F. Hill, PhD[1,2,*], Yumei Huang, PhD[3], Limei Zhu, PhD[4], Yiannos Demetriou, BS[4], Julie Ziobro, MD, PhD[5], Faith Reger, MS[1], Xiaoyan Jia, PhD[3], Joanna Mattis, MD, PhD[4], and Miriam H. Meisler, PhD[1,2]

[1]Department of Human Genetics, University of Michigan, Ann Arbor, Michigan, USA
[2]Neuroscience Graduate Program, University of Michigan, Ann Arbor, Michigan, USA
[3]Center for Genomic Technologies, Greater Bay Area Institute of Precision Medicine (Guangzhou), Fudan University, Guangzhou, Guangdong, China
[4]Department of Neurology, University of Michigan, Ann Arbor, Michigan, USA
[5]Department of Pediatrics, University of Michigan, Ann Arbor, Michigan, USA

*Current affiliation: Division of Neurology, Department of Pediatrics, Children's Hospital of Philadelphia, Philadelphia, Pennsylvania, USA

Running head: Allele-specific knockout of *Scn8a* variant (37 characters)

Word count: Abstract 133; Introduction 480; Discussion 1077; Body of manuscript 4130

Number of figures: 5

Number of tables: 1

Correspondence to:
Miriam Meisler, PhD
Department of Human Genetics
University of Michigan Medical School
4909 Buhl Box 5618
Ann Arbor MI 48109-5618
meislerm@umich.edu

This is the author manuscript accepted for publication and has undergone full peer review but has not been through the copyediting, typesetting, pagination and proofreading process, which may lead to differences between this version and the Version of Record. Please cite this article as doi: 10.1002/ana.27053

This article is protected by copyright. All rights reserved.

Author Manuscript

Author Manuscript

SUMMARY FOR SOCIAL MEDIA IF PUBLISHED

1. No twitter account.

2. Reduction of *Scn8a* transcripts by non-allele-specific ASOs can prevent seizures in *Scn8a*$^{N1768D/+}$ mice, even when initiated after seizure onset, but monthly intracranial injections were required. A few examples of allele-specific CRISPR therapies have been obtained in other mouse models.

3. Can viral delivery of an allele-specific sgRNA achieve *in vivo* editing of the dominant epileptogenic *Scn8a*^{N1768D} variant by CRISPR Cas9 in the brain?

4. Thirty percent inactivation of the pathogenic *Scn8a* transcript in brain is sufficient to rescue survival, suppress seizures, and reduce neuronal activity without adverse effects.

5. This work provides preclinical support for allele-specific genetic therapy for *SCN8A*-DEE and related syndromes.

Author Manuscript

ABSTRACT

Objective: Developmental and epileptic encephalopathies (DEEs) can result from dominant, gain of function variants of neuronal ion channels. More than 450 *de novo* missense variants of the sodium channel gene *SCN8A* have been identified in individuals with DEE.

Methods: We studied a mouse model carrying the patient *Scn8a* variant p.Asn1768Asp. An AAV-PHP.eB virus carrying an allele-specific sgRNA was administered by intracerebroventricular injection. Cas9 was provided by an inherited transgene.

Results: Allele-specific disruption of the reading frame of the pathogenic transcript generated out-of-frame indels in 1/4 to 1/3 of transcripts throughout the brain. This editing efficiency was sufficient to rescue lethality and seizures. Neuronal hyperexcitability was reduced in cells expressing the virus.

Interpretation: The data demonstrate efficient allele-specific editing of a dominant missense variant and support the feasibility of allele-specific therapy for DEE epilepsy.

Author Manuscript

INTRODUCTION

Epileptic disorders have an incidence of > 1% in the US population [1]. Variants in more than 100 genes have been associated with these disorders. One third of the identified genes encode neuronal ion channels, including the voltage-gated sodium channel genes *SCN1A*, *SCN2A*, and *SCN8A* [2]. Developmental and epileptic encephalopathy (DEE) is a severe form of epilepsy characterized by refractory seizures, SUDEP (sudden unexpected death in epilepsy), motor and gastric dysfunction, and intellectual disability [3-5]. More than 450 variants in *SCN8A* have been reported in patients with DEE [6,7].

SCN8A encodes the voltage-gated sodium channel $Na_V1.6$, which is highly enriched in the distal axon initial segment and at nodes of Ranvier and functions in initiation and propagation of action potentials [8]. Many pathogenic variants of *SCN8A* result in gain-of-function (GOF) effects on channel activity, including premature channel opening and impaired channel inactivation [3,9-11]. Expression of *Scn8a* GOF variants either in excitatory [12,13] or inhibitory neurons [14,15] can both cause seizures.

Fifty percent reduction of *Scn8a* expression by intracerebroventricular (ICV) administration of *Scn8a*-antisense oligonucleotides (ASOs) reduces seizures and extends survival [16,17]. Repeated *Scn8a*-ASO administration after seizure onset provided long-term protection to *Scn8a*-DEE mice [18]. However, limitations of ASO treatment include the need for repeated administrations and the difficulty in controlling the effect on gene expression. Reduction of *SCN8A* expression below 50% could exacerbate the deleterious effects seen in haploinsufficiency, that include intellectual disability [19,20], seizures [6,21] ataxia [22,23] and dystonia [24].

Author Manuscript

Advances in genome editing now permit allele-specific inactivation of a dominant pathogenic allele in heterozygotes. This strategy requires only a single treatment and protects the normal allele, preserving a minimum of 50% of wildtype *SCN8A* expression in cells and reducing potential adverse effects from excessive downregulation of the target gene. Successful examples of allele-specific targeting include improved hearing in mouse models of dominant deafness by delivery of sgRNA/Cas9 to the inner ear [25-27]. Allele-specific editing of the retinitis pigmentosa variant RHO^{T17M} by administration of sgRNA/Cas9 to the eye also resulted in a long-term improvement of retinal function [28].

To evaluate allele-specific editing for treatment of epilepsy, we used a mouse model carrying the dominant patient variant *Scn8a*-N1768D. This mouse line was generated by TALEN targeting, with introduction of the pathogenic A>G substitution as well as 8 nearby silent base substitutions that prevent correction of the pathogenic change [29]. This cluster of SNPs allowed us to design sgRNAs with three or four differences from the wildtype allele. (The missense variants in human *SCN8A*-DEE result from single nucleotide substitutions, only some of which can be targeted with current CRISPR/Cas9 technology.) The untreated $Scn8a^{N1768D/+}$ mice exhibit seizure onset between 2 to 3 months of age, and lethality by 5 to 6 months [16,18,30]. Here we demonstrate rescue of the disorder by allele-specific inactivation of the pathogenic allele. This result extends the feasibility of genome editing to treatment of epilepsy and other dominant neurological disorders.

Author Manuscript

METHODS

Mice: *Scn8a*$^{N1768D/+}$ (D/+) mice (JAX stock # 039107) were generated in our laboratory and maintained by backcrossing to strain C57BL/6J (JAX stock #000664) for more than 30 generations [29,30]. Mice were housed and cared for in accordance with NIH guidelines in a 12/12 hour light/dark cycle with standard mouse chow and water available *ad libitum*. Animal experiments were approved by the Institutional Animal Care and Use Committee (IACUC) at the University of Michigan in accordance with the National Institute of Health Guide for the Care and Use of Animals (Protocol #PRO00009797). Principles outlined in the ARRIVE guidelines and the Basel declaration (https://www.basel-declaration.org/) including the 3R concept have been considered when planning experiments. Cas9/Cas9 homozygous mice were purchased from the Jackson Laboratory (JAX stock #026179). D/+ mice were crossed with Cas9/Cas9 mice to generate D/+, Cas9/+ affected mice and Cas9/+ controls. Both male and female mice were used for experiments.

***In vitro* DNA digestion by Cas9:** Allele-specific DNA oligonucleotides were purchased from IDT. sgRNAs were synthesized using the EnGen sgRNA Synthesis Kit, *S. pyogenes* (NEB #3322) and purified with the Monarch RNA Cleanup Kit (NEB #T2050). SpCas9 nuclease was purchased at 1 μM concentration (NEB #M0386S). One kb DNA fragments containing the sgRNA targeted sequence were amplified by PCR from genomic DNA of wildtype or *Scn8a*$^{N1768D/N1768D}$ mice using primers F: 5'- CCC TGC TCT TTG CCT TAA T -3' and R: 5'- TTT GCC TCT TGG CTC TTT C -3'. Amplified DNA was purified with the QIAquick PCR Purification Kit (Qiagen #28106). *In vitro* DNA digestion was performed according to

manufacturer's instructions (NEB #M0386). In brief, 27 µl reactions were constituted with 1x NEBuffer r3.1, 30 nM sgRNA and 30 nM SpCas9 nuclease and incubated at 25°C for 10 minutes to permit assembly of the Cas9/sgRNA ribonucleoprotein (RNP) complex. Three µl of wildtype or *Scn8a*^{N1768D} DNA fragments (30 nM) were added and the reactions were incubated at 37°C for 15 minutes. One unit of Protease K was added to terminate the reaction and incubated at room temperature for 10 min. Reaction products were analyzed by 1.5% agarose gels.

Allele-specific editing in mouse embryonic fibroblasts (MEFs): Allele-specific sgRNA-2 and sgRNA-3 were cloned into pSpCas9(BB)-2A-Puro (PX459) V2.0 plasmid (Addgene #62988). Plasmid DNA was purified with the ZymoPURE Plasmid Miniprep Kit (Zymo #D4200). MEFs were isolated from *Scn8a*$^{N1768D/+}$ heterozygous embryos at E13.5 and grown in DMEM containing 10% FBS and 1x antibiotic antimycotic solution. After two passages, MEFs were transfected with sgRNA-expressing plasmids using Lipofectamine LTX (ThermoFisher #15338100) and selected with 2 µg/ml puromycin starting at 48 hours post transfection for 6 days. Genomic DNA was extracted and sequenced by Amplicon-EZ sequencing (Azenta, Illumina). A 482 bp DNA amplicon harboring the sgRNA targeted sequence with flanking adaptor sequence was amplified using the primer set F: 5'- ACA CTC TTT CCC TAC ACG ACG CTC TTC CGA TCT CCC TGC TCT TTG CCT TAA T -3' and R: 5'- GAC TGG AGT TCA GAC GTG TGC TCT TCC GAT CTG GCA TCA GGA TCA AAC TTC T -3'.

Analysis of Amplicon-EZ sequencing data: The adapter sequence was first trimmed from paired-end Amplicon-EZ sequencing data. The adapter-trimmed reads returned by Azenta were mapped to the 482 bp wildtype allele sequence using BWA-MEM [31]. Only read 2 files were used

Author Manuscript

for analysis since the sgRNA-targeted region is located in the middle of read 2. Then mapped paired reads were extracted from bam files using SAMtools [32] (version 1.6) followed by classification into WT-allele reads, mutant-allele reads and unclassified. To this end, the BBDuk software of BBTools (version 38.18, written by Bushnell B., https://sourceforge.net/projects/bbmap/) was used to distinguish wildtype from mutant allele based on unique sequence tags (sgRNA2-targeted samples, WT-specific tag 'CATCTCC', mutant-specific tag 'TATCTCT'; sgRNA3-targeted samples, WT-specific tag 'CTTGGAGA', mutant-specific tag 'TTTGGAGG'). Editing outcome figures were generated using CRISPResso2 [33] (version 2.2.7). Custom R scripts were further used to quantify the total indel rate and out-of-frame indel rate using output files of CRISPResso2. Out-of-frame indel rate in this study was defined as the fraction of reads whose indel size was not divisible by three.

Allele-specific editing in mouse brain: AAV-PHP.eB virus expressing the *Scn8a*^{N1768D} allele-specific sgRNA-2 paired with a BH-scaffold [34] and an eGFP fluorescent marker was prepared by the University of Michigan Vector Core. Virus (2 µl, $1x10^{13}$ vg/ml) was administered to mice by intracerebroventricular (ICV) injection at postnatal day 1 (P1). Controls received ICV administration of 2 µl PBS at P1. Brain was dissected into 6 regions (cortex, hippocampus, cerebellum, brain stem, spinal cord and remaining tissue). Total RNA was prepared by TRIzol extraction using a Direct-zol RNA Miniprep Plus Kits (Zymo #R2072). cDNA was synthesized with the LunaScript® RT SuperMix Kit (NEB #E3010L) and indels were detected by Amplicon-EZ sequencing as previously described.

Author Manuscript

Author Manuscript

Acute slice preparation and whole cell patch clamp electrophysiology: An AAV-PHP.eB virus with the eGFP cassette replaced by the red fluorescent mKATE cassette was prepared by the University of Michigan Vector Core. Virus (2 µl, $2.5x10^{13}$ vg/ml) was administered to D/+, Cas9/+ mice by ICV injection at P1. At 2-3 months post injection, mice were deeply anesthetized (via isoflurane) and brains were removed and transferred to ice-cold sucrose solution that contained, in mM: NaCl, 87; sucrose, 75; KCl, 2.5; $CaCl_2$, 1.0; $MgSO_4$, 2.0; $NaHCO_3$, 26; NaH_2PO_4, 1.25; glucose, 10) bubbled with 95% O_2 and 5% CO_2. Coronal brain slices (300 µm thickness) were prepared using a Leica VT-1200S vibratome (Leica Microsystems Inc., Buffalo Grove, IL, USA). Slices were transferred to a recording chamber containing oxygenated artificial cerebrospinal fluid (ACSF) that contained, in mM: NaCl, 125; KCl, 2.5; $CaCl_2$, 2.0; $MgSO_4$, 1.0; $NaHCO_3$, 26; NaH_2PO_4, 1.25; glucose, 10). Slices recovered at 32°C for 30 minutes and at room temperature for 30 minutes prior to recording. During recording, slices were perfused with oxygenated ACSF in a bath maintained at 31°C. Dentate gyrus granule cells were imaged using the SliceScope microscope (Scientifica) and were identified based on location within the granule cell layer. Whole cell patch clamp recordings were performed using a SliceScope Pro 6000 electrophysiology system (Scientifica). Whole cell recordings were obtained from mKATE positive and mKATE negative cells using borosilicate glass electrodes, pulled using a P-97 puller (Sutter Instruments) for a tip resistance of 3-4 MΩ. Electrodes were filled with a K-Gluconate internal solution that contained, in mM: K-gluconate, 130; KCl, 6.3; EGTA, 0.5; $MgCl_2$, 1.0; HEPES, 10; Mg-ATP, 4.0; Na-GTP, 0.3. The pH of the internal solution was adjusted to 7.30 with KOH and the osmolarity was adjusted to 285 mOsm with 30% sucrose. Electrodes were positioned via a PatchStar manipulator (Scientifica). Data were only included for final analysis if the cell had a resting potential below -70 mV. Series resistance compensation (bridge balance)

Author Manuscript

was applied throughout current clamp experiments with readjustments as necessary. No liquid junction potential correction was performed.

Analysis of whole-cell electrophysiology data: Analysis was performed blind to genotype using custom Python software and the pyABF package (https://pypi.org/project/pyabf). Action potentials (APs) were defined as passing 0 mV and having a threshold at which the derivative of the voltage (dV/dt) was greater than 10 mV/ms. Rheobase was defined as the minimum amount of current injected that resulted in at least one AP, using 1s sweeps with 20 pA intervals. AP threshold was calculated from the first AP elicited during the rheobase sweep and was defined as the first point at which the voltage rate of change was greater than 10 mV/ms. Input resistance was calculated using the change in steady state current in response to a small hyperpolarizing voltage step. AP amplitude was calculated by subtracting threshold voltage from peak voltage. The action potential duration (APD) 50 was calculated by subtracting the time of AP threshold from the time of achievement of 50% repolarization. The current/frequency plot was based on the average steady-state firing frequency calculated at each current step. The same data were used for the fold-rheobase plot by normalizing the current to each cell's rheobase and using only the integer values of fold-rheobase.

Electroencephalogram (EEG) recording: Surgical procedures were performed as previously described [17]. Simultaneous EEG recording and video monitoring were performed with a Natus recording system continuously for 14 days. Signals were acquired at 1024 Hz. Seizures and interictal background were assessed manually by an experienced reader. Interictal epileptiform discharges and seizures were defined as previously described [17,35].

Author Manuscript

RESULTS

Allele-specific targeting of the *Scn8a*^{N1768D} allele in cultured mouse embryonic fibroblasts (MEFs)

Scn8a$^{N1768D/+}$ mice (designated D/+) carry the *Scn8a* patient variant N1768D, an A to G substitution in the codon for the last residue of the S6 transmembrane segment [9]. Eight silent base substitutions were introduced nearby in the TALEN generation of the mutant mouse (Fig. 1A) [29]. Four mutant-specific sgRNAs were designed with 3 or 4 mismatches to the wildtype allele (Fig. 1A). sgRNA-2 and sgRNA-3 exhibited excellent allele-specificity in an *in vitro* DNA digestion assay (Fig. S1) and were selected for subsequent verification in tissue culture.

D/+ MEFs were isolated from E13.5 embryos and maintained in culture. sgRNA-2 and sgRNA-3 were cloned into plasmid PX459 for co-expression of SpCas9 and the puromycin resistance gene (Fig. 1B). MEFs were transfected with each plasmid and selected with puromycin, followed by genomic DNA extraction, PCR amplification and targeted next-gen sequencing. In MEFs transfected with sgRNA-2, indels were detected in 88% of the reads that mapped to the mutant allele, but only <0.5% of the reads that mapped to the wild allele, demonstrating strong allele-specificity (Fig. 1C & D). Three quarters of the indels in the mutant allele resulted in frame-shifting (Fig. 1C), generating a nearby downstream in-frame stop codon with protein truncation in the C-terminal cytoplasmic domain (Fig. 1E). Loss of this domain is known to result in loss of channel activity [36].

Author Manuscript

Transfection with sgRNA-3 plasmid also resulted in allele-specific editing of the mutant allele, but with only 16% efficiency (Fig. 1C). sgRNA-2 was selected for *in vivo* evaluation based on the higher efficiency of pathogenic allele editing in cultured MEFs.

Allele-specific editing of the *Scn8a*^{N1768D} variant in mouse brain

sgRNA-2 was packaged into AAV-PHP.eB, which preferentially transduces CNS neurons with high efficiency (Fig. 2A) [34]. D/+ mice were crossed with Cas9/Cas9 homozygotes carrying a ubiquitously expressed SpCas9 transgene [37]. D/+, Cas9/+ mice and +/+, Cas9/+ littermate controls were recovered in approximately 1:1 ratio (38:34). At postnatal day 1 (P1), D/+, Cas9/+ mice received 2 µl of AAV-PHP.eB -sgRNA-2 ($1x10^{13}$ vg/ml) virus by ICV injection. At 2 months post treatment, cDNA was prepared from brain RNA (n = 4) for targeted next-gen sequencing. Indels at the predicted Cas9 cleavage site were present in the *Scn8a*^{N1768D} allele with 25% to 34% editing efficiency in most brain regions (Fig. 2B & C, Table 1). Cerebellum had a lower editing efficiency of 16%. In the wildtype allele, the frequency of indels was less than 0.4% (Fig. 2B and Table 1). Ninety-two to 94% of indels in the mutant allele resulted in disruption of the reading frame (Fig. S2) and premature termination of translation (Fig. 2D). The edits are located in the final exon of *Scn8a*, and most edited transcripts escaped nonsense-mediated decay (Fig. S3).

Allele-specific inactivation of the *Scn8a*^{N1768D} allele protects against seizures and lethality

To assess the effect of genome editing on survival, D/+, Cas9/+ mice were treated on P1 by ICV administration of 2 µl virus. Eight of the 10 virus-treated mice survived for more than one year and are still alive (Fig. 3A). D/+, Cas9/+ mice of the control cohort received 2 µl of

PBS by ICV. Median survival of PBS-treated controls was 4 months (Fig. 3A). Thus treatment significantly extended the survival of D/+, Cas9/+ mice ($p < 0.001$, Log-rank [Mantel-Cox]test).

To examine the effect of treatment on seizure incidence, four AAV-treated D/+, Cas9/+ mice were monitored at 5-6 months of age by video/EEG recording for 14 days. Three of the four mice remained seizure-free during the recording period and the fourth exhibited a low rate of 3.5 seizures/week (Fig. 3B, C). In contrast, the five PBS-treated D/+, Cas9/+ controls exhibited frequent seizures (Fig. 3B, C), including one that experienced a terminal seizure on Day 6. The seizure phenotype in control mice was consistent with previous observations [18,30]. Seizure frequency was significantly reduced by AAV treatment (Fig. 3C). The percent of seizure-free mice increased from 0/5 in PBS-treated mice to 3/4 in the AAV-treated mice ($p < 0.05$, Chi-Square test). Targeted inactivation of the pathogenic allele was protective against both seizures and lethality.

Inactivation of the *Scn8a*^{N1768D} allele reduces excitability in dentate gyrus granule cells

Previous studies identified elevated neuronal activity in several types of neurons from D/+ mice, including hippocampal CA1 and CA3 neurons [13], dentate gyrus granule cells[38] , and medial entorhinal cortex neurons [39]. We investigated the effect of editing on electrophysiological properties of dentate gyrus granule cells, since their activation can influence seizure susceptibility [40], and they exhibit differentially expressed genes after chronic seizures [38]. Mice with genotype D/+, Cas9/+ were treated on P1 by ICV injection of the AAV.PHP.eB-sgRNA-2 virus carrying the mKATE cassette which expresses a red fluorescent marker. Acute brain slices were prepared two months after treatment. Transduced (mKATE positive) neurons were identified by their red fluorescence and recorded to determine whether viral infection had altered

Author Manuscript

Author Manuscript

their intrinsic excitability. Nearby non-transduced neurons (mKATE negative) in the same slices were recorded as negative controls. mKATE positive granule cells had a significantly higher rheobase compared to mKATE negative cells, likely due to lower input resistance as opposed to higher action potential threshold (Fig. 4A-C). In mKATE positive cells, the amplitude of the first action potential was increased to 81.4 ± 1.2 mV compared with 72.2 ± 3.4 mV in mKATE negative cells ($p = 0.03$). The action potential duration (APD) 50 was reduced to 1.01 ± 0.02 msec in the transduced cells compared with 1.07 ± 0.03 sec ($p = 0.001$) in non-transduced cells. A similar increase in the duration of the action potential was previously seen in hippocampal CA1 neurons of D/+ mice relative to wildtype[13]. In response to small current injections, mKATE positive granule cells fired fewer action potentials, as seen in example traces (Fig. 4D) and in the right-shifted current/frequency (I-f) plot (Fig. 4E). Normalizing the I-f plot to rheobase (Fig. 4F) eliminated the right-shift, suggesting that this difference was attributable to the higher rheobase of transduced mKATE positive granule cells. (A significant difference persisted in response to larger current injections.) Thus intrinsic neuronal excitability was reduced by transduction with the sgRNA-2 virus.

Assessment of movement in mice with reduced expression of pathogenic *Scn8a*^{N1768D} allele

To detect potential deleterious effects of *Scn8a* editing, D/+, Cas9/+ and +/+, Cas9 littermates were treated with AAV-PHP.eb-sgRNA-2 on P1 and examined at 6 months of age for behavior in the open field test. The two groups did not differ in distance traversed, average velocity, or time at rest in the open field (Fig. 5A).

In previous studies, the D/+ mice did not exhibit a motor phenotype in the open field test [30]. Reduction of *Scn8a* expression to 50% of wildtype level by ASO did not cause motor deficits

in these mice [16,18]. In this study, the 30% editing in the D/+ mice also failed to impair motor function. There were no signs of failure to thrive as a result of the reduced expression of the *Scn8a*^{N1768D} allele, and bodyweight was unaffected at six months of age (Fig. 5B). Thus AAV-PHP.eB mediated *Scn8a*^{N1768D} allele inactivation was well tolerated.

DISCUSSION

We examined the efficacy of allele-specific editing of the dominant epileptogenic variant *Scn8a*^{N1768D} by CRISPR/Cas9 in brain. Neuronal targeting was achieved using the AAV-PHP.eB virus and allele specificity was based on several mismatches between *Scn8a*^{N1768D} and the wildtype allele. Viral delivery of an allele-specific sgRNA generated out-of-frame indels predominantly in the mutant allele, achieving 25-34% editing efficiency throughout the cerebrum and spinal cord, with lower efficiency (16%) in cerebellum. This effect was sufficient to rescue survival and suppress seizures in the mutant mice, without obvious adverse effects. Our results demonstrate that allele-specific inactivation of pathogenic *Scn8a* alleles is attainable in the brain of a heterozygous variant at a sufficient frequency to rescue seizures and lethality.

Scn8a is broadly expressed in neurons throughout the CNS and PNS. Precision medicine for GOF variants of *Scn8a* must achieve a sufficient reduction in expression to ameliorate the major pathology without the detrimental side effects of $Na_V1.6$ deficiency [41-43]. A significant advantage of allele-specific targeting is that the maximum reduction of expression is 50%, preventing the development of more severe adverse effects than those seen with haploinsufficiency.

Author Manuscript

Author Manuscript

After ICV administration of the AAV-PHP.eB virus, editing efficiency was high throughout the brain. Previous studies demonstrated the importance of cortex and hippocampus in GOF *Scn8a* epilepsy. For example, expression of the GOF *Scn8a*^{R1872W} in forebrain excitatory neurons was sufficient to induces seizures and sudden death [12]. There is elevated activity in hippocampal CA1, CA3 and granule neurons from *Scn8a*-DEE mice [12,38]. Downregulation of *Scn8a*^{N1768D} expression in the dentate gyrus region of the hippocampus by an *Scn8a*-shRNA extended survival in D/+ mice [38]. Hyperexcitability was also reported in entorhinal cortex neurons from D/+ mice [39]. These studies suggest that inactivation of the *Scn8a*^{N1768D} allele in cortex and hippocampus contributes to the positive outcome. Despite the epileptic phenotype, untreated D/+ mice do not exhibit impaired motor function. In the current work the cerebellum had somewhat lower editing efficiency of 16% that did not lead to obvious adverse effects on motor function. The cerebellum has limited surface area contacting the fourth ventricle, which likely resulted in less efficient diffusion of virus. The effect of 30% editing in brain stem and remaining tissues remain to be studied.

It is interesting to compare this work with our previous administration of an ASO complementary to the 3' untranslated region of the *Scn8a* transcript [16]. The ASO rescued survival by reducing the overall abundance of *Scn8a* transcript to 50% of normal, with comparable effect predicted for both alleles. In comparison, allele-specific CRISPR/Cas9 targeting rescued survival with only 25% editing of the mutant transcript, or 12% reduction of functional *Scn8a* transcripts. Thus, the allele-specific treatment could be considered more efficient.

Inactivation of the *Scn8a*^{N1768D} allele in between 1/4 to 1/3 of neurons was sufficient to prevent seizures and lengthen survival in our studies. How does allele-specific inactivation achieve seizure protection *in vivo*? CRISPR/Cas9 editing of the pathogenic allele deletes the C-

terminal domain of the channel protein and generates a functionally null allele [36,44]. Neurons with inactivation of the pathogenic variant express a single active wildtype allele. When comparing the intrinsic excitability of AAV-PHP.eB-sgRNA-2 transduced (mKATE positive) and non-transduced (mKATE negative) granule cells, we found that transduced cells had significantly higher rheobase compared to adjacent non-transduced granule cells patched within the same slices. In other words, the amount of current required to depolarize the transduced granule cells to action potential threshold was significantly higher than non-transduced cells. Thus, the cells with loss of the GOF channel were hypoexcitable compared with the non-transduced neurons. This effect likely contributes to seizure reduction *in vivo*.

Previous work identified decreased rheobase in neurons expressing pathogenic GOF *Scn8a* variants such as p.(Arg223Gly) [45], p.(R1872W) [11], and p.(N1768D) [14]. Further study will be required to elucidate the precise mechanism by which *Scn8a* editing contributes to increased rheobase in granule cells, and the generalizability of our granule cell data to other cell types and brain regions. In a previous study, we reported a significant increase of firing frequency in D/+ dentate gyrus granule cells, with no difference in rheobase or individual properties of the first AP at rheobase [38]. In the current study, knock-out of the mutant N1768D allele decreased firing frequency but also changed rheobase and AP waveforms. The haploinsufficiency of *Scn8a* in edited cells might contribute to these changes. It is also possible that partial reduction of $Na_v1.6$ expression causes elevated expression of $Na_v1.2$ channels, as previously shown in null cortical pyramidal neurons [46]. The mechanism by which reduced excitability of 25% of neurons disrupts circuit hypersynchrony remains to be determined.

The allele-specific CRISPR-Cas9 (CRISPRi) editing described here utilized a cluster of 3 base mismatches in the sgRNA between wildtype and mutant alleles. However, most human

Author Manuscript

Author Manuscript

pathogenic alleles contain a single nucleotide substitution, which can only be targeted with current CRISPR/Cas9 if the substitution generates a new protospacer adjacent motif (PAM) site or is located very close to the PAM site of the sgRNA. In addition, CRISPRi inactivation of the mutant allele involves a double-stranded break in chromosomal DNA with potential deleterious off-target effects. Clinical application will require different gene-editing technology, such as base editing or prime editing. Base editing has good editing efficiency and allele specificity but the targeted base must be located in the editing window determined by the matching PAM site. Base editors may also produce undesired bystander edits since all suitable bases within the editing window could be modified potentially generating new mutations. Prime editing avoids bystander editing but has low editing efficiency. Our demonstration of the efficacy of allele-specific inactivation of 1/4 to 1/3 of a dominant *SCN8A* variant demonstrates 'proof of principle' for efforts to develop base editing and prime editing therapies for *SCN8A*-DEE and related disorders.

Despite the introduction of many new antiepileptic drugs in the past thirty years, approximately one third of patients remain drug-resistant. Several hundred different *SCN8A* variants have been described in patients with DEE, varying in functional deficit and causing a spectrum of clinical severity [3,4,10,11]. The level of editing required for a therapeutic response may depend on the functional effect of each variant. Many individuals with *SCN8A*-DEE experience unremitting seizures, sleep and gastric disturbances, and elevated risk of SUDEP [4,6]. Thus, even partial therapeutic efficacy could be valuable. Genetic therapies that reduce expression of GOF *Scn8a* variants, using ASOs or CRISPRi, are effective in preventing seizures and prolonging healthy life in mouse models of DEE. Translation of these preclinical observations to clinical applications is an urgent priority for the future.

Author Manuscript

ACKNOWLEDGEMENTS

This work was supported by NINDS grants R01-NS34509 to MHM, K08-NS121464 to JM and K08-NS124937 to JZ. The AAV-PHP.eB viruses expressing *Scn8a* sgRNAs were prepared in the University of Michigan Vector Core (Thomas Lanigan, Director).

AUTHOR CONTRIBUTIONS

W.Y., and M.H.M. contributed to the conception and design of the study; W.Y., S.F.H., Y.H., L.Z., Y.D., J.Z., and F.R. contributed to the acquisition and analysis of data; W.Y., Y.H., X.J., J.M., and M.H.M. contributed to drafting the text and preparing figures.

POTENTIAL CONFLICTS OF INTEREST

The authors report no potential conflicts of interest.

DATA AVAILABILITY

All relevant data is included in the manuscript.

Author Manuscript

REFERENCES

1 Zack, M. M. & Kobau, R. National and State Estimates of the Numbers of Adults and Children with Active Epilepsy - United States, 2015. *MMWR Morb Mortal Wkly Rep* **66**, 821-825 (2017). https://doi.org:10.15585/mmwr.mm6631a1

2 Guerrini, R., Conti, V., Mantegazza, M. *et al.* Developmental and epileptic encephalopathies: from genetic heterogeneity to phenotypic continuum. *Physiol Rev* **103**, 433-513 (2023). https://doi.org:10.1152/physrev.00063.2021

3 Meisler, M. H., Helman, G., Hammer, M. F. *et al.* SCN8A encephalopathy: Research progress and prospects. *Epilepsia* **57**, 1027-1035 (2016). https://doi.org:10.1111/epi.13422

4 Johannesen, K. M., Gardella, E., Encinas, A. C. *et al.* The spectrum of intermediate SCN8A-related epilepsy. *Epilepsia* **60**, 830-844 (2019). https://doi.org:10.1111/epi.14705

5 Sanders, S. J., Campbell, A. J., Cottrell, J. R. *et al.* Progress in Understanding and Treating SCN2A-Mediated Disorders. *Trends Neurosci* **41**, 442-456 (2018). https://doi.org:10.1016/j.tins.2018.03.011

6 Johannesen, K. M., Liu, Y., Koko, M. *et al.* Genotype-phenotype correlations in SCN8A-related disorders reveal prognostic and therapeutic implications. *Brain* **145**, 2991-3009 (2022). https://doi.org:10.1093/brain/awab321

7 Hu, C., Luo, T. & Wang, Y. Phenotypic and genetic spectrum in Chinese children with SCN8A-related disorders. *Seizure* **95**, 38-49 (2022). https://doi.org:10.1016/j.seizure.2021.12.011

8 Meisler, M. H., Hill, S. F. & Yu, W. Sodium channelopathies in neurodevelopmental disorders. *Nat Rev Neurosci* **22**, 152-166 (2021). https://doi.org:10.1038/s41583-020-00418-4

9 Veeramah, K. R., O'Brien, J. E., Meisler, M. H. *et al.* De novo pathogenic SCN8A mutation identified by whole-genome sequencing of a family quartet affected by infantile epileptic encephalopathy and SUDEP. *Am J Hum Genet* **90**, 502-510 (2012). https://doi.org:10.1016/j.ajhg.2012.01.006

10 Vanoye, C. G., Abramova, T. V., DeKeyser, J. M. *et al.* Molecular and Cellular Context Influences SCN8A Variant Function. *bioRxiv* (2023). https://doi.org:10.1101/2023.11.11.566702

11 Liu, Y., Schubert, J., Sonnenberg, L. *et al.* Neuronal mechanisms of mutations in SCN8A causing epilepsy or intellectual disability. *Brain* **142**, 376-390 (2019). https://doi.org:10.1093/brain/awy326

12 Bunton-Stasyshyn, R. K. A., Wagnon, J. L., Wengert, E. R. *et al.* Prominent role of forebrain excitatory neurons in SCN8A encephalopathy. *Brain* **142**, 362-375 (2019). https://doi.org:10.1093/brain/awy324

13 Lopez-Santiago, L. F., Yuan, Y., Wagnon, J. L. *et al.* Neuronal hyperexcitability in a mouse model of SCN8A epileptic encephalopathy. *Proc Natl Acad Sci U S A* **114**, 2383-2388 (2017). https://doi.org:10.1073/pnas.1616821114

14 Wengert, E. R., Miralles, R. M., Wedgwood, K. C. A. *et al.* Somatostatin-Positive Interneurons Contribute to Seizures in SCN8A Epileptic Encephalopathy. *J Neurosci* **41**, 9257-9273 (2021). https://doi.org:10.1523/JNEUROSCI.0718-21.2021

15 Miralles, R. M., Boscia, A. R., Kittur, S. *et al.* Parvalbumin Interneuron Impairment Leads to Synaptic Transmission Deficits and Seizures in SCN8A Epileptic Encephalopathy. *bioRxiv* (2024). https://doi.org:10.1101/2024.02.09.579511

Author Manuscript

16 Lenk, G. M., Jafar-Nejad, P., Hill, S. F. *et al.* Scn8a Antisense Oligonucleotide Is Protective in Mouse Models of SCN8A Encephalopathy and Dravet Syndrome. *Ann Neurol* **87**, 339-346 (2020). https://doi.org:10.1002/ana.25676

17 Hill, S. F., Ziobro, J. M., Jafar-Nejad, P. *et al.* Genetic interaction between Scn8a and potassium channel genes Kcna1 and Kcnq2. *Epilepsia* **63**, e125-e131 (2022). https://doi.org:10.1111/epi.17374

18 Hill, S. F., Yu, W., Ziobro, J. *et al.* Long-term downregulation of the sodium channel gene Scn8a is therapeutic in mouse models of SCN8A epilepsy. *Ann Neurol* (2023). https://doi.org:10.1002/ana.26861

19 Wagnon, J. L., Barker, B. S., Ottolini, M. *et al.* Loss-of-function variants of SCN8A in intellectual disability without seizures. *Neurol Genet* **3**, e170 (2017). https://doi.org:10.1212/NXG.0000000000000170

20 Wengert, E. R., Tronhjem, C. E., Wagnon, J. L. *et al.* Biallelic inherited SCN8A variants, a rare cause of SCN8A-related developmental and epileptic encephalopathy. *Epilepsia* **60**, 2277-2285 (2019). https://doi.org:10.1111/epi.16371

21 Blanchard, M. G., Willemsen, M. H., Walker, J. B. *et al.* De novo gain-of-function and loss-of-function mutations of SCN8A in patients with intellectual disabilities and epilepsy. *J Med Genet* **52**, 330-337 (2015). https://doi.org:10.1136/jmedgenet-2014-102813

22 Trudeau, M. M., Dalton, J. C., Day, J. W. *et al.* Heterozygosity for a protein truncation mutation of sodium channel SCN8A in a patient with cerebellar atrophy, ataxia, and mental retardation. *J Med Genet* **43**, 527-530 (2006). https://doi.org:10.1136/jmg.2005.035667

23 Lyu, H., Bosselmann, C. M., Johannesen, K. M. *et al.* Clinical and electrophysiological features of SCN8A variants causing episodic or chronic ataxia. *EBioMedicine* **98**, 104855 (2023). https://doi.org:10.1016/j.ebiom.2023.104855

24 Kearney, J. A., Buchner, D. A., De Haan, G. *et al.* Molecular and pathological effects of a modifier gene on deficiency of the sodium channel Scn8a (Na(v)1.6). *Hum Mol Genet* **11**, 2765-2775 (2002). https://doi.org:10.1093/hmg/11.22.2765

25 Gyorgy, B., Nist-Lund, C., Pan, B. *et al.* Allele-specific gene editing prevents deafness in a model of dominant progressive hearing loss. *Nat Med* **25**, 1123-1130 (2019). https://doi.org:10.1038/s41591-019-0500-9

26 Gao, X., Tao, Y., Lamas, V. *et al.* Treatment of autosomal dominant hearing loss by in vivo delivery of genome editing agents. *Nature* **553**, 217-221 (2018). https://doi.org:10.1038/nature25164

27 Tao, Y., Lamas, V., Du, W. *et al.* Treatment of monogenic and digenic dominant genetic hearing loss by CRISPR-Cas9 ribonucleoprotein delivery in vivo. *Nat Commun* **14**, 4928 (2023). https://doi.org:10.1038/s41467-023-40476-7

28 Liu, X., Qiao, J., Jia, R. *et al.* Allele-specific gene-editing approach for vision loss restoration in RHO-associated retinitis pigmentosa. *Elife* **12** (2023). https://doi.org:10.7554/eLife.84065

29 Jones, J. M. & Meisler, M. H. Modeling human epilepsy by TALEN targeting of mouse sodium channel Scn8a. *Genesis* **52**, 141-148 (2014). https://doi.org:10.1002/dvg.22731

30 Wagnon, J. L., Korn, M. J., Parent, R. *et al.* Convulsive seizures and SUDEP in a mouse model of SCN8A epileptic encephalopathy. *Hum Mol Genet* **24**, 506-515 (2015). https://doi.org:10.1093/hmg/ddu470

31 Li, H. Aligning sequence reads, clone sequences and assembly contigs with BWA-MEM. *arXiv* (2013). https://doi.org:10.48550/arXiv.1303.3997

Author Manuscript

32 Danecek, P., Bonfield, J. K., Liddle, J. *et al.* Twelve years of SAMtools and BCFtools. *Gigascience* **10** (2021). https://doi.org:10.1093/gigascience/giab008

33 Clement, K., Rees, H., Canver, M. C. *et al.* CRISPResso2 provides accurate and rapid genome editing sequence analysis. *Nat Biotechnol* **37**, 224-226 (2019). https://doi.org:10.1038/s41587-019-0032-3

34 Hana, S., Peterson, M., McLaughlin, H. *et al.* Highly efficient neuronal gene knockout in vivo by CRISPR-Cas9 via neonatal intracerebroventricular injection of AAV in mice. *Gene Ther* **28**, 646-658 (2021). https://doi.org:10.1038/s41434-021-00224-2

35 Kao, H. Y., Hu, S., Mihaylova, T. *et al.* Defining the latent period of epileptogenesis and epileptogenic zone in a focal cortical dysplasia type II (FCDII) rat model. *Epilepsia* **62**, 1268-1279 (2021). https://doi.org:10.1111/epi.16868

36 Mantegazza, M., Yu, F. H., Catterall, W. A. & Scheuer, T. Role of the C-terminal domain in inactivation of brain and cardiac sodium channels. *Proc Natl Acad Sci U S A* **98**, 15348-15353 (2001). https://doi.org:10.1073/pnas.211563298

37 Platt, R. J., Chen, S., Zhou, Y. *et al.* CRISPR-Cas9 knockin mice for genome editing and cancer modeling. *Cell* **159**, 440-455 (2014). https://doi.org:10.1016/j.cell.2014.09.014

38 Yu, W., Hill, S. F., Zhu, L. *et al.* Dentate gyrus granule cells are a locus of pathology in Scn8a developmental encephalopathy. *(in revision)* (2024).

39 Ottolini, M., Barker, B. S., Gaykema, R. P. *et al.* Aberrant Sodium Channel Currents and Hyperexcitability of Medial Entorhinal Cortex Neurons in a Mouse Model of SCN8A Encephalopathy. *J Neurosci* **37**, 7643-7655 (2017). https://doi.org:10.1523/JNEUROSCI.2709-16.2017

40 Mattis, J., Somarowthu, A., Goff, K. M. *et al.* Corticohippocampal circuit dysfunction in a mouse model of Dravet syndrome. *Elife* **11** (2022). https://doi.org:10.7554/eLife.69293

41 Burgess, D. L., Kohrman, D. C., Galt, J. *et al.* Mutation of a new sodium channel gene, Scn8a, in the mouse mutant 'motor endplate disease'. *Nat Genet* **10**, 461-465 (1995). https://doi.org:10.1038/ng0895-461

42 Levin, S. I. & Meisler, M. H. Floxed allele for conditional inactivation of the voltage-gated sodium channel Scn8a (NaV1.6). *Genesis* **39**, 234-239 (2004). https://doi.org:10.1002/gene.20050

43 Meisler, M. H., Kearney, J., Escayg, A. *et al.* Sodium channels and neurological disease: insights from Scn8a mutations in the mouse. *Neuroscientist* **7**, 136-145 (2001). https://doi.org:10.1177/107385840100700208

44 Jones, J. M., Dionne, L., Dell'Orco, J. *et al.* Single amino acid deletion in transmembrane segment D4S6 of sodium channel Scn8a (Nav1.6) in a mouse mutant with a chronic movement disorder. *Neurobiol Dis* **89**, 36-45 (2016). https://doi.org:10.1016/j.nbd.2016.01.018

45 Liu, Y., Koko, M. & Lerche, H. A SCN8A variant associated with severe early onset epilepsy and developmental delay: Loss- or gain-of-function? *Epilepsy Res* **178**, 106824 (2021). https://doi.org:10.1016/j.eplepsyres.2021.106824

46 Katz, E., Stoler, O., Scheller, A. *et al.* Role of sodium channel subtype in action potential generation by neocortical pyramidal neurons. *Proc Natl Acad Sci U S A* **115**, E7184-E7192 (2018). https://doi.org:10.1073/pnas.1720493115

Author Manuscript

FIGURE LEGENDS

Figure 1. Editing of the *Scn8a*^{N1768D} allele in heterozygous *Scn8a*$^{N1768D/+}$ MEF cells. (**A**) The *Scn8a*^{N1768D} causal mutation is an A to G substitution at residue 1768 (shown in red). The N1768D allele was designed with eight additional silent base substitutions (blue) within 50 bp of the pathogenic mutation. Four sgRNAs were designed specific for the mutant allele containing 3 or 4 mismatches to the wildtype allele (yellow). The PAM sequence is shown in bold. (**B**) PX459 vector insert for sgRNA expression. (**C**) Allele-specific editing of the *Scn8a*^{N1768D} allele in heterozygous D/+ MEF cells. Editing efficiency of sgRNA-2 and sgRNA-3. The sequencing depth of control, sgRNA-2, and sgRNA3 experiments were $4.6x10^5$, $2.6x10^5$, and $5.2x10^5$ respectively. (**D**) Graphic representation of indels from MEFs transfected with sgRNA-2 plasmid. Three silent base substitutions in the sgRNA that mark the mutant allele are indicated by red triangles. The A to G substitution causing *Scn8a*-N1768D is in red box. *Sequence identical to the corresponding reference sequences; base substitutions are shown in bold; deletions are represented by dashes. (**E**) Indels in the mutant allele generated in-frame stop codons and truncation of the C-terminal protein domain which is known to inactivate the channel [36]. The pathogenic D residue is shown in red.

Figure 2. Editing of the *Scn8a*^{N1768D} allele in mouse brain. (A) AAV-PHP.eB viral construct for sgRNA-2 expression. **(B)** Editing efficiency in AAV-PHP.eB treated D/+, Cas9/+ mouse brain (n = 4). The sequencing depth for each experiment group was between $4x10^5$ to $16x10^5$. (**C**) Indels from cortex of an AAV-PHP.eB treated D/+, Cas9/+ mouse. The silent base substitutions in the sgRNA that are specific for the mutant allele are marked by red triangles. A to G

substitution causing the *Scn8a*-N1768D mutation is underlined. *Sequence identical to the corresponding reference sequences. Bold: substitutions; box: insertions; -: deletions. (**D**) Indels in the mutant allele resulted in generation of in-frame stop codons and truncation of C-terminal protein sequence. The pathogenic D residue is shown in red.

Figure 3. Allele-specific inactivation of the *Scn8a*^{N1768D} allele rescues lethality and seizures. (**A**) Survival. D/+, Cas9/+ mice were treated by ICV administration on P1 with AAV-PHP.eB-sgRNA-2 or PBS (*** $p < 0.001$, Log-rank [Mantel-Cox]test). (**B**) Seizures. Mice were monitored for two weeks by continuous video/EEG monitoring. Representative traces from each animal were recorded by right and left epidural electrodes. Left: Three out of four D/+, Cas9/+ mice that received AAV treatment were completely protected from electrographic and convulsive seizures; the fourth AAV-treated mouse had occasional seizures. Right: Control D/+, Cas9/+ mice received PBS and exhibited both electrographic and behavioral seizures. * Death during recording. (**C**) Seizure frequency. (** $p < 0.01$, unpaired t-test).

Figure 4. Cellular effects of editing: decreased excitability in transduced dentate gyrus granule cells. Mice were injected ICV on P1 with the AAV-PHP.eB-sgRNA-2 virus expressing the red fluorescent mKATE marker and recordings were made from transduced (red fluorescent) and non-transduced dentate gyrus granule cells (GCs)**.** (**A**) The rheobase of transduced (mKATE^{+}) cells (red) (162±18 pA) was significantly higher than that of non-transduced (mKATE^{-}) cells (blue) (66±6 pA). (**B**) mKATE^{+} and mKATE^{-} cells had a similar action potential threshold. (**C**) The input resistance of transduced mKATE^{+} GCs was reduced to almost half that of mKATE^{-} GCs (183±18 vs. 359±31 MOhm). (**D**) Representative current clamp recordings of evoked action potentials elicited by increasing current injections from GCs. (**E**) The current/frequency (I-f) plot for transduced mKATE^{+} GCs (red) was right-shifted, reflecting the higher rheobase. (**F**) I-f plot with current normalized to the rheobase of each class of cells. The curve for transduced mKATE^{+} cells

Author Manuscript

(red) had a similar rise and faster decay compared with mKATE$^-$ GCs. GCs were recorded from 4 mice; n = 14 mKATE$^+$, n = 14 mKATE$^-$. **** p = < 0.0001; unpaired t-test (**A-C**) or 2-way ANOVA (**E-F**). Line and shaded areas represent mean and SEM.

Figure 5. Open field test of D/+, Cas9/+ mice after allele-specific editing. D/+, Cas9/+ mice (n = 5) and +/+, Cas9/+ littermates (n = 6) were treated with AAV-PHP.eB-sgRNA-2 virus at P1. At 6 months of age, behavior in the open field test was monitored for 15 min on 4 successive days. **(A-C)** The activity of treated mutant mice did not differ significantly from treated control mice. (**D**) Absence of deleterious impact of viral treatment is indicated by normal body weight of mice at 6 months of age, compared with untreated wildtype mice. Mean ± SD.

Author Manuscript

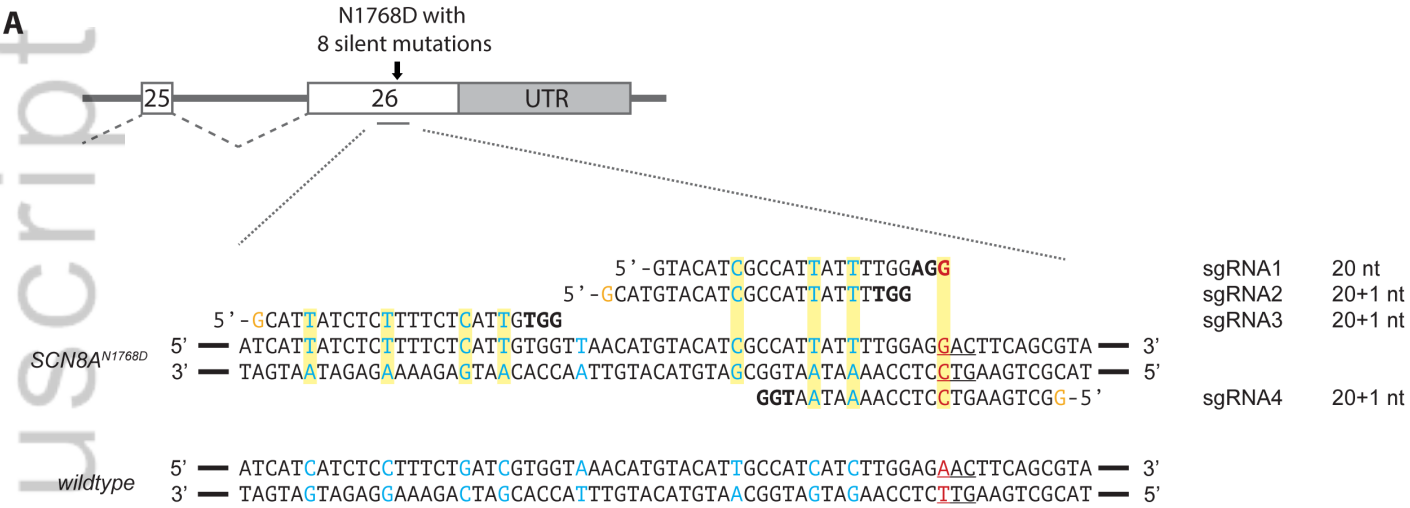
Table 1. Editing efficiency of the *Scn8a*^{N1768D} and wildtype alleles in heterozygous brain.
D/+, Cas9/+ mice received ICV injection of AAV-PHP.eB-sgRNA-2 virus at P1. Two months later, RNA was extracted from 6 brain regions and converted to cDNA. The editing efficiency of the *Scn8a*^{N1768D} allele (**A**) and the wildtype allele (**B**) were determined by Amplicon-EZ next-gen sequencing. Each column represents one animal.

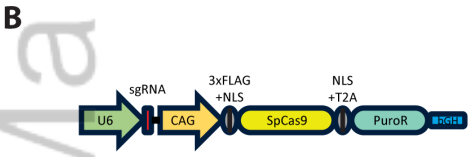
A	Editing efficiency of the *Scn8a*^{N1768D} allele: % of reads with indels				
Brain region	#1	#2	#3	#4	Mean ± SD
Cortex	31%	26%	30%	36%	30 ± 4%
Hippocampus	24%	22%	24%	29%	25 ± 3%
Cerebellum	15%	13%	15%	22%	16 ± 4%
Brain stem	28%	27%	29%	28%	28 ± 1%
Spinal cord	35%	35%	35%	19%	31 ± 8%
Residual	36%	38%	36%	24%	34 ± 6%

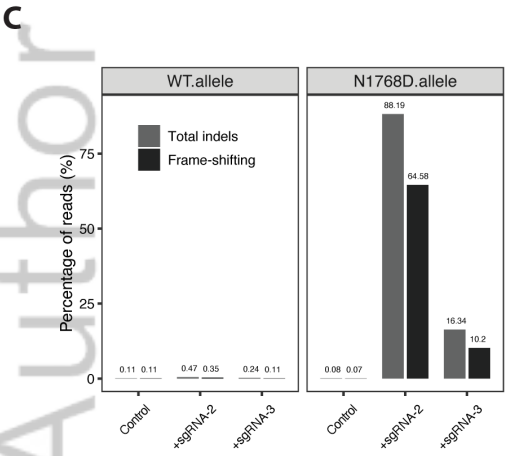
B	Editing efficiency of the wildtype allele: % of reads with indels				
Brain region	#1	#2	#3	#4	Mean ± SD
Cortex	0.37%	0.34%	0.27%	0.34%	0.33 ± 0.04%
Hippocampus	0.33%	0.34%	0.24%	0.26%	0.3 ± 0.05%
Cerebellum	0.24%	0.24%	0.24%	0.33%	0.26 ± 0.05%
Brain stem	0.35%	0.34%	0.31%	0.26%	0.31 ± 0.04%
Spinal cord	0.42%	0.41%	0.34%	0.19%	0.34 ± 0.11%
Residual	0.45%	0.45%	0.39%	0.2%	0.37 ± 0.12%

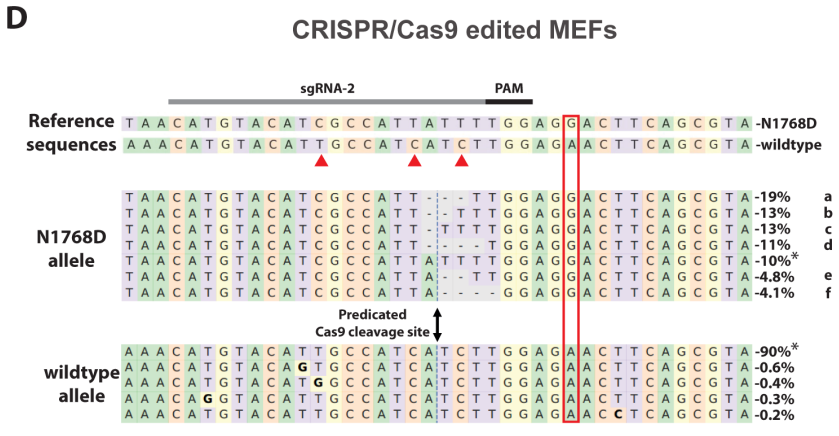
Author Manuscript

Author Manuscript









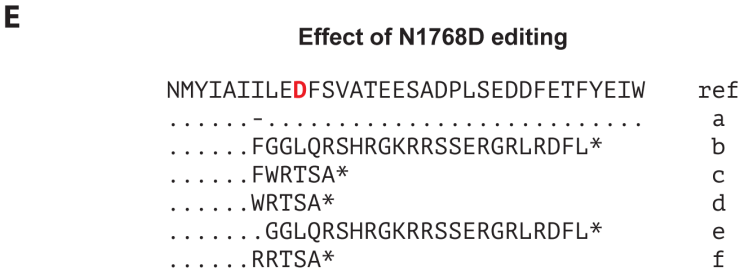


Fig 1 RGB ver2.tif

Author Manuscript

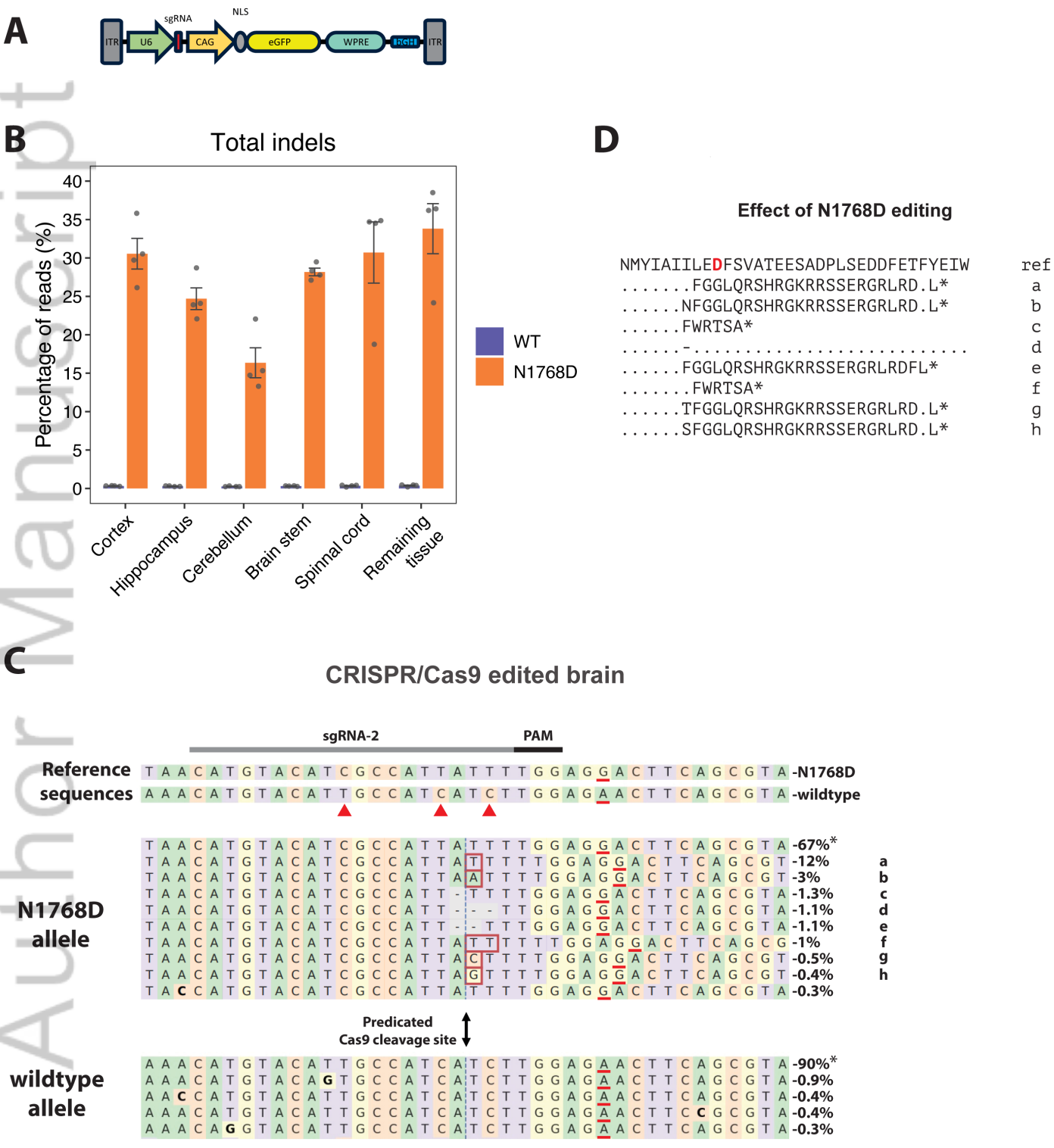
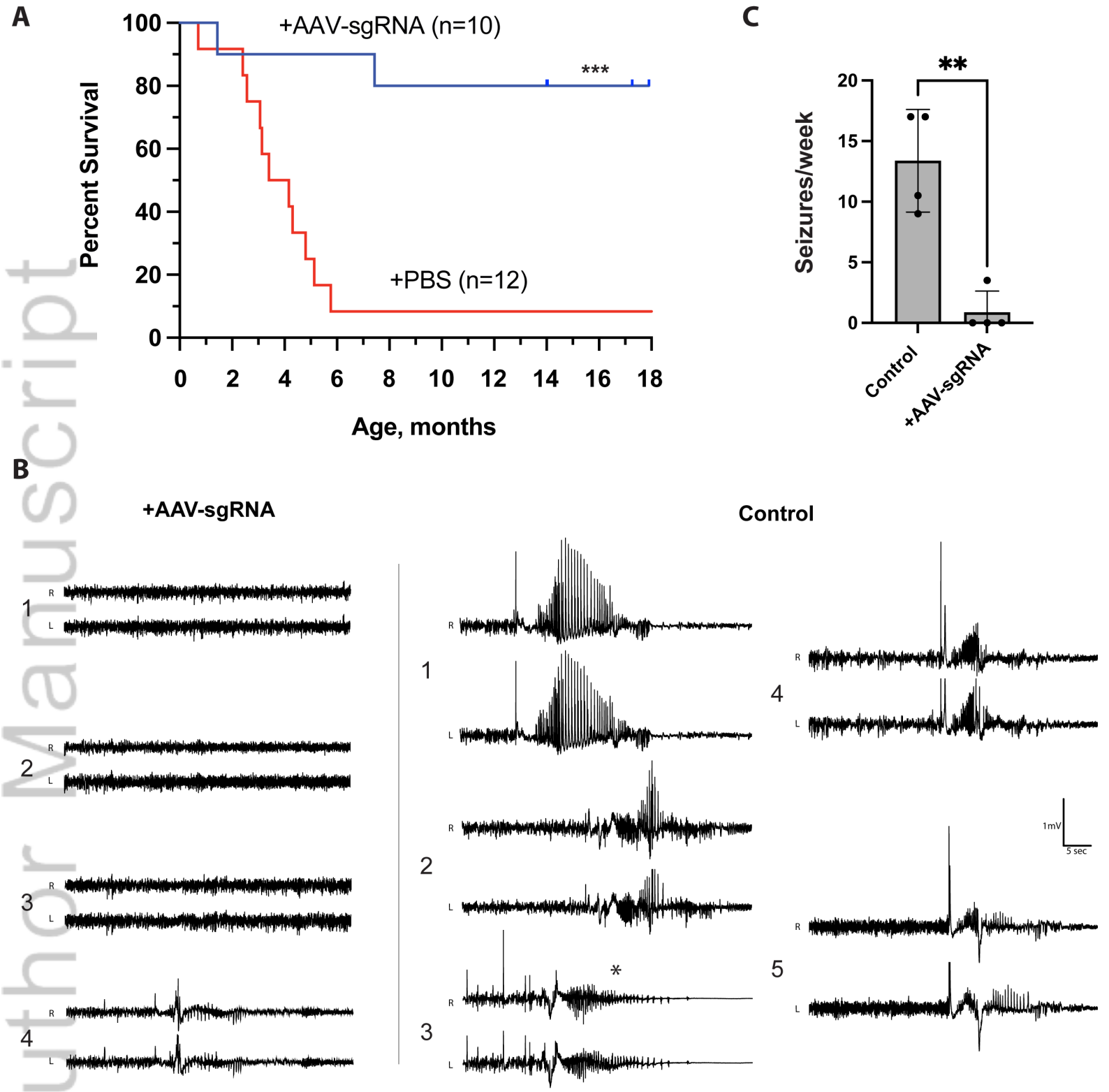


Fig 2 RGB ver2.tif



Author Manuscript

Fig 3 RGB ver2.tif

Author Manuscript

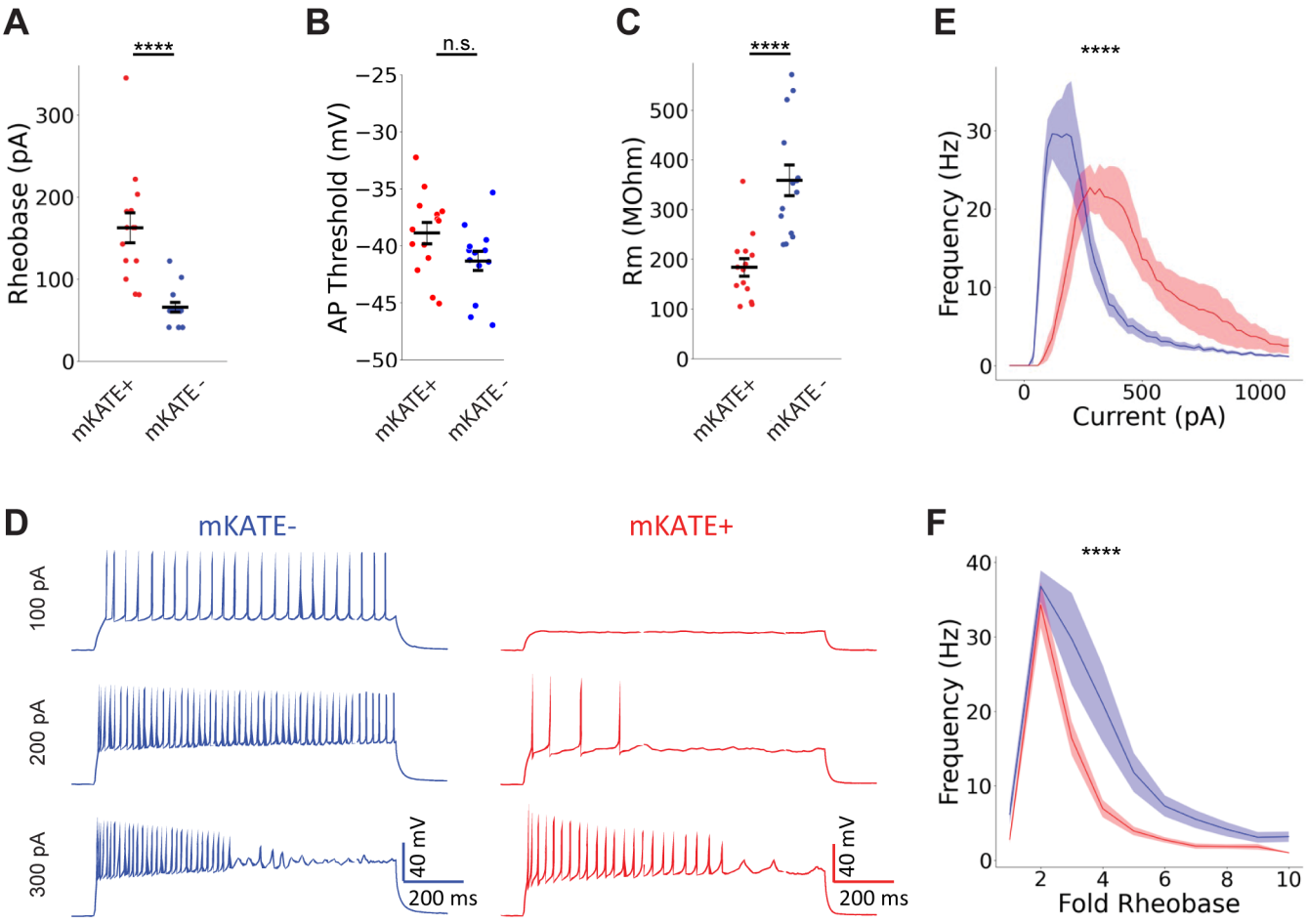


Fig 4 RGB ver2.tif

Author Manuscript

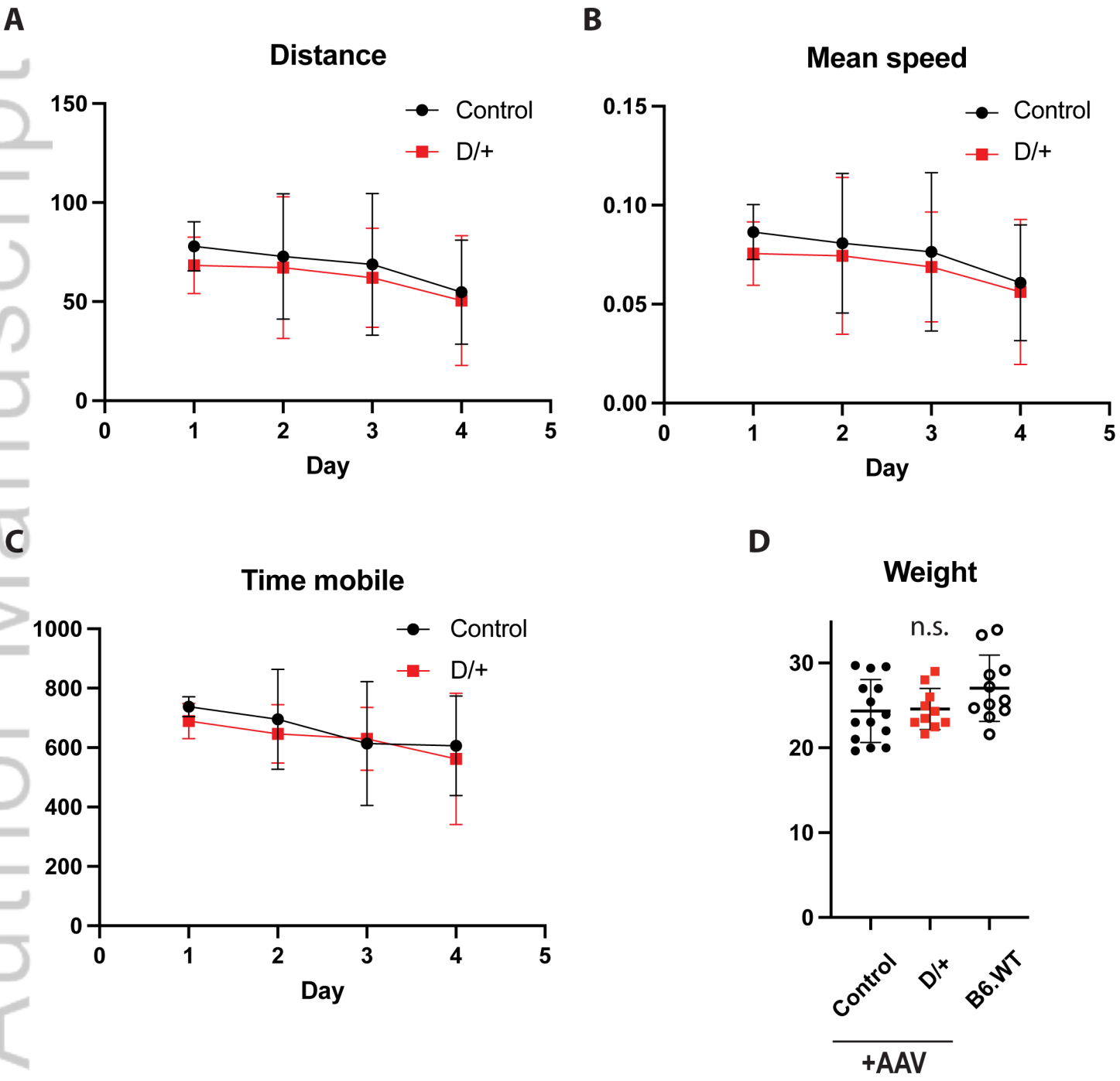


Fig 5.tif

Author Manuscript

Table 1. Editing efficiency of the *Scn8a*^{N1768D} and wildtype alleles in heterozygous brain.
D/+, Cas9/+ mice received ICV injection of AAV-PHP.eB-sgRNA-2 virus at P1. Two months later, RNA was extracted from 6 brain regions and converted to cDNA. The editing efficiency of the *Scn8a*^{N1768D} allele (**A**) and the wildtype allele (**B**) were determined by Amplicon-EZ next-gen sequencing. Each column represents one animal.

A	Editing efficiency of the *Scn8a*^{N1768D} allele: % of reads with indels				
Brain region	#1	#2	#3	#4	Mean ± SD
Cortex	31%	26%	30%	36%	30 ± 4%
Hippocampus	24%	22%	24%	29%	25 ± 3%
Cerebellum	15%	13%	15%	22%	16 ± 4%
Brain stem	28%	27%	29%	28%	28 ± 1%
Spinal cord	35%	35%	35%	19%	31 ± 8%
Residual	36%	38%	36%	24%	34 ± 6%

B	Editing efficiency of the wildtype allele: % of reads with indels				
Brain region	#1	#2	#3	#4	Mean ± SD
Cortex	0.37%	0.34%	0.27%	0.34%	0.33 ± 0.04%
Hippocampus	0.33%	0.34%	0.24%	0.26%	0.3 ± 0.05%
Cerebellum	0.24%	0.24%	0.24%	0.33%	0.26 ± 0.05%
Brain stem	0.35%	0.34%	0.31%	0.26%	0.31 ± 0.04%
Spinal cord	0.42%	0.41%	0.34%	0.19%	0.34 ± 0.11%
Residual	0.45%	0.45%	0.39%	0.2%	0.37 ± 0.12%